

Spectroscopic signature of trimer Mott insulator and charge disproportionation in BaIrO₃

R. Okazaki^{1,*}, S. Ito², K. Tanabe^{2,†}, H. Taniguchi², Y. Ikemoto³, T. Moriwaki³, and I. Terasaki²

¹*Department of Physics, Faculty of Science and Technology, Tokyo University of Science, Noda 278-8510, Japan*

²*Department of Physics, Nagoya University, Nagoya 464-8602, Japan and*

³*SPRING-8, Japan Synchrotron Radiation Research Institute (JASRI), Sayo, Hyogo 679-5198, Japan*

We have measured the reflectivity spectra of the barium iridate 9R BaIrO₃, the crystal structure of which consists of characteristic Ir₃O₁₂ trimers. In the high-temperature phase above the transition temperature $T_c \approx 180$ K, we find that the optical conductivity involves two temperature-dependent optical transitions with an ill-defined Drude response. These features are reminiscent of the optical spectra in the organic dimer Mott insulators, implying a possible emergence of an unusual electronic state named trimer Mott insulator in BaIrO₃, where the carrier is localized on the trimer owing to the strong Coulomb repulsion. Along with a pronounced splitting of the phonon peak observed below T_c , which is a hallmark of charge disproportionation, we discuss a possible phase transition from the trimer Mott insulator to a charge-ordered insulating phase in BaIrO₃.

I. INTRODUCTION

Recent observations of exotic electronic states in 4*d*- and 5*d*-electron systems, such as unusual orbital ordering in ruthenates [1–3] and the spin-orbit Mott insulator in iridates [4–7], have emphasized the emergent physics of correlated electron systems. In contrast to well-localized 3*d* orbital, 4*d* and 5*d* electrons have extended electronic wave functions, making the Coulomb repulsion comparable to the bandwidth. These energy scales also compete with spin-orbit interactions, leading to intriguing spin-orbital-entangled electronic states in those materials.

Another important aspect of the 4*d*- and 5*d*-electron systems with spatial extent of the *d* orbitals is close coupling with the lattice degrees of freedom. A representative unit structure in the transition-metal oxides is MO₆ octahedron (M being transition-metal ion), which tends to form a corner-shared network like the perovskite structure as seen in various 3*d* oxides. On the other hand, in 4*d* and 5*d* oxides, the network structures made of edge- and face-sharing octahedra also become stable owing to the direct hybridization among the extended *d* orbitals. Interestingly, such compounds exhibit anomalous phase transitions related to a molecular orbital formation of *d* orbitals, such as a metal-insulator transition in Li₂RuO₃ driven by a dimerization of edge-sharing RuO₆ octahedra [8, 9] and an antiferromagnetic transition in Ba₄Ru₃O₁₀ related to a molecular orbital formation in Ru₃O₁₂ trimers made of face-sharing octahedra [10, 11].

9R phase BaIrO₃ is particularly unique among them, since it exhibits an intriguing quasi-one-dimensional crystallographic form and an unconventional phase transition at $T_c \approx 180$ K, below which a weak ferromagnetism and a gap opening simultaneously set in [12–16]. The crystal structure is composed of Ir₃O₁₂ trimers, made up of three face-sharing IrO₆ octahedra as depicted in the inset of Fig. 1(a) [12]. Note that the Ir-Ir distance in the trimer is shorter than that of Ir metal, indicating a strong hybridization of the intra-trimer 5*d* orbitals. The corner-sharing trimers form a zig-zag chain along the *c* axis [12]. The quasi-one-dimensional nature also appears in the anisotropic transport properties [15, 17].

The issue to be addressed is how the structural feature correlates with the origin of the phase transition at T_c . Var-

ious measurements including resistivity [15], magnetoresistance [18], thermopower [17, 19], optical spectroscopy [15], and photoemission [20], suggest a (partial) gap opening in the density of states below T_c , indicating a charge-density-wave (CDW) formation as is expected from the low-dimensional crystal structure. This is supported by tight-binding and local-spin-density approximation calculations [21, 22], which also suggest an itinerant ferromagnetism within a Stoner picture. On the other hand, the CDW model is not straightforward because the nonmetallic transport behaviors are reported both above and below T_c [15, 17, 19], and to our knowledge, there is no experimental evidence for the appearance of the superlattice reflections accompanying the CDW formation below T_c [23, 24]. Furthermore, the significance of spin-orbit interaction is also suggested [25, 26], complicating the underlying mechanism of the phase transition.

In this study, we present the detailed temperature variation of the optical conductivity spectra of BaIrO₃ to grasp the electronic structure in a wide energy range. Above T_c , we find that the optical conductivity spectra possess a qualitative similarity to that of the organic dimer Mott insulators, in which the correlated carrier is localized on the dimerized molecules to act as a Mott insulator. Thus this result indicates a molecular orbital formation of 5*d* orbitals in the Ir₃O₁₂ trimers and a possible emergence of an unusual electronic state named trimer Mott insulator, where the carrier is localized on the trimer by the Coulomb repulsion, as is suggested by recent structural investigation [24]. Below T_c , the optical phonon peaks further split, indicating an occurrence of a charge disproportionation. Based on the present results, we discuss an inter-trimer charge degree of freedom to drive a phase transition from the trimer Mott to a charge order insulator.

II. EXPERIMENTS

Single-crystalline samples of BaIrO₃ with a typical dimension of $0.3 \times 0.3 \times 1$ mm³ were grown by the self-flux method [17]. Powders of IrO₂ (99.9%) and BaCl₂ (99.9%) were mixed in a molar ratio of 1 : 10. The mixture was put in an alumina crucible and heated up to 1523 K in air with a heating rate of 200 K/h. After keeping 1523 K for 12 h, it was slowly cooled

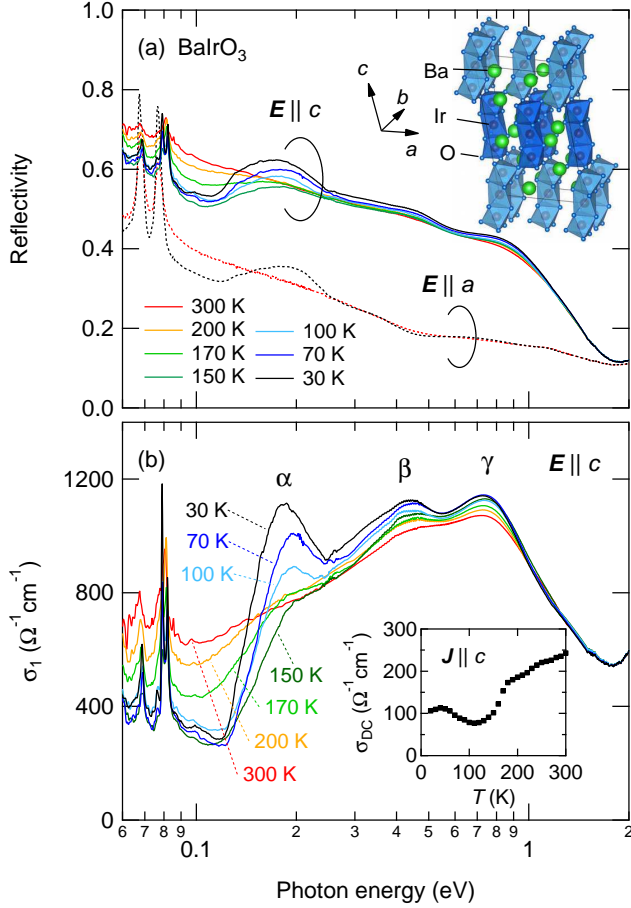


FIG. 1. (Color online). (a) Reflectivity spectra measured at several temperatures with polarization parallel to the c axis (solid curves) and the a axis (dotted curves). The inset depicts the crystal structure of $9R$ BaIrO_3 . Light- and dark-blue colors show the inequivalent Ir_3O_{12} trimers. (b) Optical conductivity spectra measured with polarization parallel to the c axis. The inset shows the temperature dependence of the dc conductivity along the c axis taken from Ref. 17.

down with a rate of 1 K/h, and at 1123 K the power of the furnace was switched off. The crystal axis was determined by Laue method.

The polarized reflectivity spectra were measured using a Fourier transform infrared spectrometer (FTIR) with a synchrotron radiation (SR) light at BL43IR, SPring-8, Japan for energies between 60 meV and 1.0 eV [27], an FTIR (FTIR-6000 and IRT-5000, JASCO Corp.) for energies between 0.2 eV and 1.4 eV, and a grating spectrometer for energies between 1.2 eV and 2.5 eV. For the infrared range from 60 meV to 1.4 eV, we used a helium flow-type refrigerator and the sample was fixed with a silver paste on the cold head. Here we used a standard gold overcoating technique for measuring the reference spectrum at each temperature. For the visible range, we have only performed room-temperature measurement and used a SiC for the reference [28]. The complex optical conductivity is obtained from the Kramers-Kronig (KK) analysis. We used a constant extrapolation of the reflectivity up to 6 eV

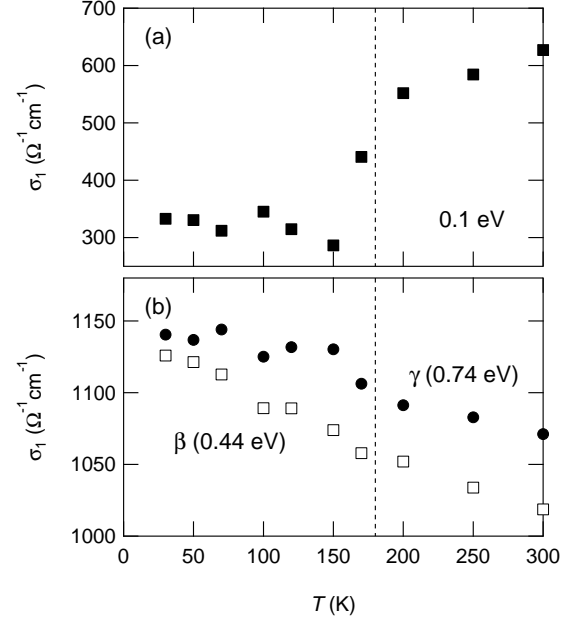


FIG. 2. (a) Temperature dependence of the low-energy optical conductivity at $\hbar\omega = 0.1$ eV. The dashed line represents the transition temperature $T_c \approx 180$ K. (b) Temperature variations of the optical conductivity at the β peak (open squares) and the γ peak (filled circles).

and subsequently employed a standard extrapolation of ω^{-4} dependence. In low energies, we extrapolated the reflectivity using several methods, but the influence on the peak shapes and positions is negligible for discussion.

III. RESULTS AND DISCUSSION

A. Reflectivity and optical conductivity

Figure 1(a) shows the temperature variation of the reflectivity spectra. The reflectivity measured with the polarization parallel to the c axis (solid curves) is significantly larger than that for a -axis (dotted curves), consistent with the transport anisotropy [15, 17]. Note that earlier optical experiments used unpolarized light above 0.74 eV [15], which may result in worse KK transformation. Hereafter we focus on the optical data for the conducting c axis.

The reflectivity spectra exhibit a considerable temperature dependence. Above T_c , the optical phonon structures below 0.1 eV are unscreened and the low-energy reflectivity decreases with lowering temperature, indicating a nonmetallic high-temperature phase. In the infrared range, we notice three temperature-dependent peak structures around 0.2, 0.4, and 0.7 eV, which will be discussed in the optical conductivity spectra. On the other hand, the temperature dependence becomes small and converges around 1 eV. Thus we used the room-temperature data for the reflectivity spectra of all temperatures above 1.4 eV as mentioned in the previous session

and the discussion on the temperature variation will be restricted only below 1 eV.

Figure 1(b) depicts the real part of the optical conductivity spectra σ_1 . We find three temperature-dependent peak structures labelled as α (~ 0.2 eV), β (~ 0.4 eV), γ (~ 0.7 eV) in the infrared range, and the temperature variations of the optical conductivity at several characteristic photon energies are shown in Figs. 2. In contrast to the present result, the optical conductivity of $J_{\text{eff}} = 1/2$ Mott insulator Sr_2IrO_4 involves two characteristic peaks below 1 eV [29], implying intrinsically different electronic structures among these iridates.

B. High-temperature phase above T_c

First we discuss the high-temperature electronic state. As shown in Figs. 1(b) and 2(a), above T_c , the optical conductivity in the low-energy region around 0.1 eV is gradually suppressed with lowering temperature. Moreover, as shown in the inset of Fig. 1(b), the DC conductivity σ_{DC} [17], which equals to $\sigma_1(\omega \rightarrow 0)$, is smaller than the optical conductivity in the low-energy range. These results clearly demonstrate a nonmetallic nature in the high-temperature phase of BaIrO_3 , consistent with the nonmetallic transport [15, 17, 19] and the localized electronic state [20] even above T_c . The temperature dependence of the optical conductivity at 0.1 eV [Fig. 2(a)] is qualitatively similar to that of DC conductivity [inset of Fig. 1(b)], indicating that the transport properties are strongly affected by the electronic structure in a wide energy range.

To further understand the insulating nature above T_c , we then discuss the origins of the temperature-dependent peaks observed in the infrared range. Now we consider a localized picture of Ir $5d$ electrons proposed in Ref. 24. As schematically drawn in Figs. 3(a) and (b), one Ir^{4+} ion has the electronic configuration of $5d^5$ in the triply-degenerate t_{2g} orbital, which further splits into higher a_{1g} and lower doubly-degenerate e'_g orbitals owing to a trigonal distortion.

An important point is that BaIrO_3 consists of the Ir_3O_{12} trimers in which the Ir-Ir distance is fairly short. We then consider a molecular orbital formation between three a_{1g} orbitals within a trimer, and obtain bonding (B), non-bonding (NB), and anti-bonding (AB) orbitals as shown in Figs. 3(c) and (d). In this case, we find one electron in the NB orbital, and this state can be regarded as half-filling if we identify one trimer as one structural unit. In this picture, we may assign the highest γ peak as the transition between B and NB orbitals (trimer peak), which is good agreement with the estimation of ~ 1 eV by the band calculation [25]. Also, the transition between NB and AB orbitals, in which the energy difference is close to that of the B-NB transition, is also included in the γ peak. Note that the transition from B to AB orbitals is prohibited in a simple dipole transition since both orbitals have even parity. Furthermore, as depicted in Fig. 3(e), in the presence of the Coulomb interaction, this half-filled state can become a Mott insulator, which can explain the insulating behaviors mentioned above, and the transition between the lower- and upper-Hubbard bands may be assigned as the β peak.

Strong spin-orbit interaction, essential for understanding

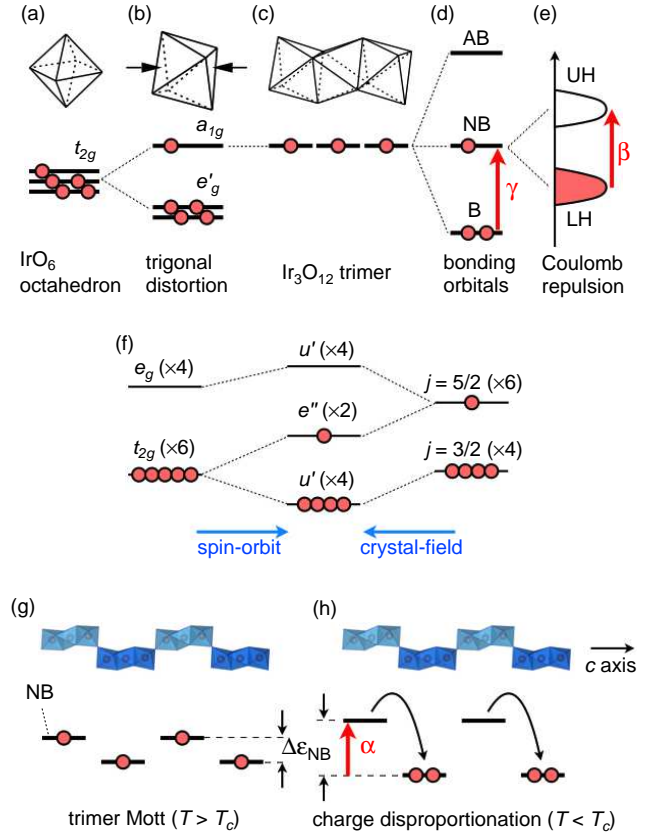


FIG. 3. (Color online). Schematic energy diagrams for the electronic state of BaIrO_3 constructed from a localized picture [24]. The red arrows labelled as α , β , γ correspond to the optical transitions shown in Fig. 1(b). Energy diagrams for Ir $5d$ electrons in (a) IrO_6 octahedron, (b) trigonally distorted octahedron, (c) Ir_3O_{12} trimer. (d) In the trimer, three a_{1g} orbitals form the bonding (B), non-bonding (NB), and anti-bonding (AB) orbitals. (e) Under strong correlation effect, the half-filled NB orbitals split into lower-Hubbard (LH) and upper-Hubbard (UH) bands. (f) Energy levels for Ir^{4+} under spin-orbit and crystal-field interactions [26]. (g) Trimer Mott insulating state realized above $T_c \approx 180$ K. The energy difference of NB orbitals between two inequivalent trimers is relatively small. (h) Charge disproportionation below T_c .

electronic states of iridates [4, 5], can be taken in the present model. As depicted in Fig. 3(f), under spin-orbit and crystal-field interactions, the $5d$ states split into highest quadruply-degenerate u' , doubly-degenerate e'' , and lowest quadruply-degenerate u' levels, and the highest-occupied level is the e'' level as is suggested by x-ray absorption study [26]. However, even in such a case, the e'' level instead of the a_{1g} level may form molecular orbitals in the trimer, and thus the situation to realize the half-filled NB state is unaltered.

The present insulating state can be called trimer Mott insulator [24], in analogy to the dimer Mott insulator, in which a correlated carrier is localized on the dimerized organic molecules to act as a Mott insulator [30]. Indeed, the optical conductivity of BaIrO_3 has a similarity to that of the dimer Mott insulator: It also involves a transition between bonding

and anti-bonding orbitals in a dimer (dimer peak) and a transition between Hubbard bands [31]. Moreover, the intensities of these optical transitions increase with lowering temperature [32], also similar to the enhancements of β - and γ -peak intensities with cooling as shown in Fig. 2(b). Note that these intensities contrastingly decrease with lowering temperature to enhance the Drude weight in correlated metallic state [32]. Thus the present results of the optical conductivity above T_c may capture the essential features of a trimer Mott insulator state in the high-temperature phase of BaIrO_3 .

A schematic picture of the trimer Mott insulator state above T_c is drawn in Fig. 3(g). The correlated carrier is localized at each NB orbital, which is formed by the a_{1g} or the e'' levels. Note that there are two crystallographically-inequivalent trimers [12], and the energy difference between the NB orbitals of these trimers $\Delta\epsilon_{\text{NB}}$ may be small above T_c .

C. Low-temperature phase below T_c

Having the above arguments in mind, let us discuss the low-temperature electronic state below T_c . The distinct feature below T_c is an enhancement of the α peak shown in Fig. 1(b), which is reminiscent of those in CDW compounds [33] and in charge order systems [34, 35], indicating that a similar electronic state emerges in the low-temperature phase of BaIrO_3 . Here the trimer Mott insulator state discussed above is unstable against the charge order (charge disproportionation), because one must have finite energy difference between the two NB levels of crystallographically-inequivalent trimers ($\Delta\epsilon_{\text{NB}} \neq 0$). Thus, as shown in Fig. 3(h), if $\Delta\epsilon_{\text{NB}}$ is relatively large, a carrier is transferred from the high- to the low-energy NB level, leading to a charge disproportionation. Indeed, recent x-ray diffraction study using synchrotron radiation has revealed that the two trimers become more inequivalent with lowering temperature [24], supporting the charge disproportionation scenario. In this case, the α peak corresponds to the transition between two NB levels with the energy difference $\Delta\epsilon_{\text{NB}}$. Note that the low-temperature enhancement of the α peak is also observed clearly in the reflectivity measured with the polarization parallel to the a axis [Fig. 1(a)], consistent with the gap opening for the charge disproportionation below T_c .

In order to examine this scenario, we focus on the phonon spectra, which are sensitive to the charge disproportionation [36]. As plotted in Fig. 4(a), we find two temperature-dependent peaks around 80 meV, which may be assigned as stretching modes of IrO_6 [29], although the thorough assignment is incomplete. We then try to fit these spectra with two Lorentz oscillators,

$$\sigma_1(\omega) = \epsilon_0 \omega \sum_{k=1}^2 \omega_{p,k}^2 \frac{\gamma_k \omega}{(\omega_k^2 - \omega^2)^2 + \gamma_k^2 \omega^2}, \quad (1)$$

where ϵ_0 is the electric constant and $\omega_{p,k}$, ω_k , and γ_k are the plasma frequency, the resonance frequency, and the damping factor of the k th oscillator, respectively. In Fig. 4(a), the fitting results of each oscillator and the sum are shown by the dashed

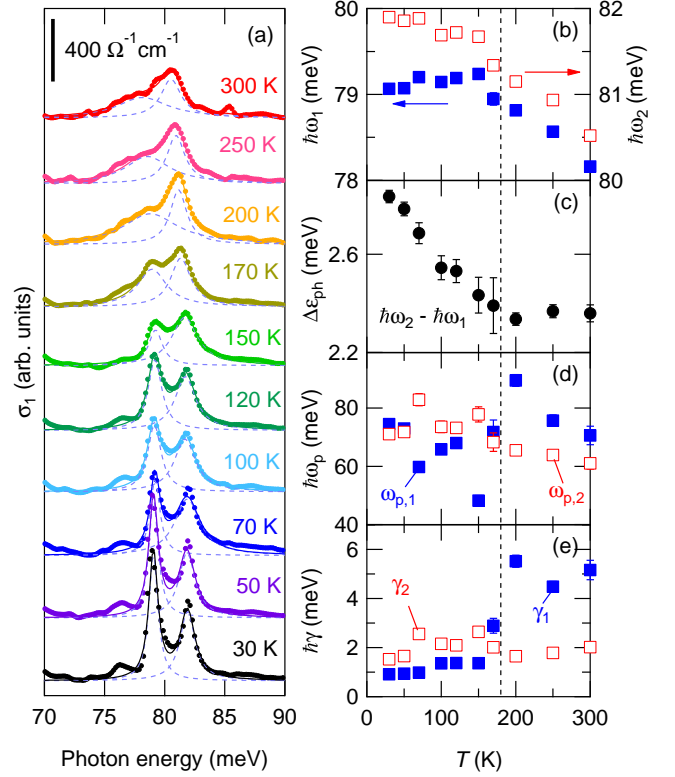


FIG. 4. (Color online). (a) Optical phonon spectra measured at several temperatures with polarization parallel to the c axis. The experimental data are fitted using two Lorentz oscillators shown as the dashed curves for each temperature. The sum of two oscillators is represented as the solid curves. (b-e) Temperature variations of the fitting parameters; (b) the resonance energies at around $\hbar\omega_1 \approx 79$ meV (solid squares, left axis) and $\hbar\omega_2 \approx 81$ meV (open squares, right axis), (c) the difference of the resonance energies $\Delta\epsilon_{\text{ph}} = \hbar\omega_2 - \hbar\omega_1$, (d) the plasma frequencies, and (e) the damping factors. The vertical dashed line represents the transition temperature $T_c \approx 180$ K.

and the solid curves, respectively. The two-oscillators fitting well reproduces the experimental results below and above T_c , indicating no translational symmetry breaking at T_c , consistent with the earlier diffraction studies [23, 24]. Note that a very small peak around 76 meV, which is not taken account of in this fitting, does not affect the results.

Figures 4(b) and 4(c) show the temperature variations of the resonance energies $\hbar\omega_k$ ($k = 1, 2$) and the difference $\Delta\epsilon_{\text{ph}} = \hbar\omega_2 - \hbar\omega_1$, respectively. Below T_c , $\Delta\epsilon_{\text{ph}}$ dramatically increases with decreasing temperature, similar to the phonon peak splitting in the charge order phase in oxides [37] and organic systems [35, 38]. Whereas a critical difference is that the charge-order compounds exhibit translational symmetry breaking while the present iridate does not, the increase of $\Delta\epsilon_{\text{ph}}$ below T_c indeed suggests that a charge imbalance is pronouncedly enhanced in the low-temperature phase. Here there are four crystallographically-inequivalent Ir sites in the unit cell (i.e. central and edge Ir sites for two inequivalent

trimers), but a NB nature with no central weight of the wave function indicates that the edge IrO_6 octahedra are more sensitive to the amount of charge rather than the central one. Indeed, the theoretical calculation has shown that the density of states of the central Ir ions in the trimers is suppressed at the Fermi energy [21], which is naturally understood within the NB nature. Therefore the enhancement of $\Delta\epsilon_{\text{ph}}$ may reflect a difference of charge amounts between the edge Ir sites of the inequivalent trimers, indicating an inter-trimer charge disproportionation shown in Fig. 3(h). We note that, in opposite to this charge disproportionation among the NB orbitals, the β peak, which reflects the feature of the trimer Mott state in the NB orbital, is negligibly affected and enhanced even at low temperatures as shown in Fig. 2(b). This possibly implies that the amount of inter-trimer charge difference is small, similarly to some charge-ordered organic compounds with small difference in the site charge $\Delta\rho < 0.1e$ [39]. Nevertheless, the concurrent observation of the phonon peak splitting and the α peak growth below T_c has a striking similarity to that of charge-ordered organic salts [34, 35, 38], strongly indicating an emergence of the charge disproportionation.

Temperature variations of the plasma frequencies $\hbar\omega_{p,k}$ and the damping factors $\hbar\gamma_k$ ($k = 1, 2$) are shown in Fig. 4(d) and 4(e), respectively. While these data are scattering, we find that $\hbar\gamma_1$ is anomalously enhanced above T_c , as is clearly seen in the high-temperature phonon spectra in Fig. 4(a). Such a broadening is also reported in the high-temperature phase of the organic charge order systems and is considered as a fluctuation of the charge order [40]. Thus the phonon peak broadening at high temperatures in BaIrO_3 possibly indicates a fluctuation or a precursor of the charge disproportionation.

We finally mention the low-energy optical conductivity, which is suppressed but a finite weight remains even below T_c [Figs. 1(b) and 2(a)]. This result suggests a pseudogap formation, as is consistent with the optical and photoemission studies [15, 20]. Such a pseudogap behavior has also

been observed in the optical conductivity of BaRuO_3 , which possesses a Ru_3O_{12} trimer [41]. We infer that, since the organic dimer Mott insulator competes with the charge order phase [35], the trimer Mott insulator and charge-transferred state proposed above may compete with each other to generate such a pseudogap behavior.

IV. SUMMARY

In summary, the optical conductivity measurements on BaIrO_3 single crystals shed light on the unconventional phase transition at $T_c \approx 180$ K in this trimer-based compound. Above T_c , the optical conductivity spectra clearly show an insulating behavior and a qualitative similarity to that of the organic dimer Mott insulators, indicating an importance of the molecular orbital formation among $5d$ orbitals in the trimer and a possible emergence of the trimer Mott insulator. Below T_c , we find further splitting of the optical phonon peaks, indicating an occurrence of a charge disproportionation. The present results emphasize an inter-trimer charge degree of freedom to drive a phase transition from the trimer Mott to charge order insulator in BaIrO_3 , and may offer a fascinating playground to investigate the physics of *inorganic* molecular solids.

ACKNOWLEDGEMENTS

We thank J. Akimitsu and T. Arima for valuable comments. The experiments using synchrotron radiation were performed at BL43IR in SPring-8 with the approvals of JASRI (No. 2014B1116, No. 2015A1189). This work was supported by the JSPS KAKENHI (No. 25610091, No. 26287064, No. 26610099, No. 17H06136, No. 18K13504).

* Email: okazaki@rs.tus.ac.jp

† Present address: Toyota Technological Institute, Nagoya 468-8511, Japan

- [1] S. A. J. Kimber, J. A. Rodgers, H. Wu, C. A. Murray, D. N. Argyriou, A. N. Fitch, D. I. Khomskii, and J. P. Attfield, *Phys. Rev. Lett.* **102**, 046409 (2009).
- [2] S. Kunkemöller, D. Khomskii, P. Steffens, A. Piovano, A. A. Nugroho, and M. Braden, *Phys. Rev. Lett.* **115**, 247201 (2015).
- [3] A. Jain, M. Krautloher, J. Porras, G. H. Ryu, D. P. Chen, D. L. Abernathy, J. T. Park, A. Ivanov, J. Chaloupka, G. Khaliullin, B. Keimer, and B. J. Kim, *Nat. Phys.* **13**, 633-637 (2017).
- [4] B. J. Kim, Hosub Jin, S. J. Moon, J.-Y. Kim, B.-G. Park, C. S. Leem, Jaejun Yu, T. W. Noh, C. Kim, S.-J. Oh, J.-H. Park, V. Durairaj, G. Cao, and E. Rotenberg, *Phys. Rev. Lett.* **101**, 076402 (2008).
- [5] B. J. Kim, H. Ohsumi, T. Komesu, S. Sakai, T. Morita, H. Takagi, and T. Arima, *Science* **323**, 1329 (2009).
- [6] G. Jackeli and G. Khaliullin, *Phys. Rev. Lett.* **102**, 017205 (2009).
- [7] K. Kitagawa, T. Takayama, Y. Matsumoto, A. Kato, R. Takano, Y. Kishimoto, S. Bette, R. Dinnebier, G. Jackeli, and H. Takagi, *Nature* **554**, 341-345 (2018).
- [8] Y. Miura, Y. Yasui, M. Sato, N. Igawa, and K. Kakurai, *J. Phys. Soc. Jpn.* **76**, 033705 (2007).
- [9] I. Terasaki, S. Abe, Y. Yasui, R. Okazaki, and H. Taniguchi, *J. Mater. Chem. C* **3**, 10430 (2015).
- [10] T. Igarashi, Y. Nogami, Y. Klein, G. Rousse, R. Okazaki, H. Taniguchi, Y. Yasui, and I. Terasaki, *J. Phys. Soc. Jpn.* **82**, 104603 (2003).
- [11] T. Igarashi, R. Okazaki, H. Taniguchi, Y. Yasui, and I. Terasaki, *J. Phys. Soc. Jpn.* **84**, 094601 (2015).
- [12] T. Siegrist and B. L. Chamberland, *J. Less Common Met.* **170**, 93-99 (1991).
- [13] A. V. Powell and P. D. Battle, *J. Alloys Comp.* **191**, 313-318 (1993).
- [14] R. Lindsay, W. Strange, B. Chamberland, and R. Moyer, *Solid State Commun.* **86**, 759-763 (1993).
- [15] G. Cao, J.E. Crow, R.P. Guertin, P.F. Henning, C.C. Homes, M. Strongin, D.N. Basov, E. Lochner, *Solid State Commun.* **113**,

- 657-662 (2000).
- [16] M. L. Brooks, S. J. Blundell, T. Lancaster, W. Hayes, F. L. Pratt, P. P. C. Frampton, and P. D. Battle, *Phys. Rev. B* **71**, 220411(R) (2005).
 - [17] T. Nakano and I. Terasaki, *Phys. Rev. B* **73**, 195106 (2006).
 - [18] G. Cao, X. N. Lin, S. Chikara, V. Durairaj, and E. Elhami, *Phys. Rev. B* **69**, 174418 (2004).
 - [19] N. Kini, A. Bentien, S. Ramakrishnan, and C. Geibel, *Physica B* **359-361**, 1264-1266 (2005).
 - [20] K. Maiti, R. S. Singh, V. R. R. Medicherla, S. Rayaprol, and E. V. Sampathkumaran, *Phys. Rev. Lett.* **95**, 016404 (2005).
 - [21] M. H. Whangbo and H. J. Koo, *Solid State Commun.* **118**, 491 (2001).
 - [22] K. Maiti, *Phys. Rev. B* **73**, 115119 (2006).
 - [23] S. Shinohara, S. Mori, T. Nakano, and I. Terasaki, *Abstr. Meet. Physical Society of Japan (62nd Annu. Meet., 2007)*, Part 3, p. 582, 22aWF-9 [in Japanese].
 - [24] I. Terasaki, S. Ito, T. Igarashi, S. Asai, H. Taniguchi, R. Okazaki, Y. Yasui, K. Kobayashi, R. Kumai, H. Nakao, and Y. Murakami, *Crystals* **6**, 27 (2016).
 - [25] Weiwei Ju, Guo-Qiang Liu, and Zhongqin Yang, *Phys. Rev. B* **87**, 075112 (2013).
 - [26] M. A. Laguna-Marco, D. Haskel, N. Souza-Neto, J. C. Lang, V. V. Krishnamurthy, S. Chikara, G. Cao, and M. van Veenendaal, *Phys. Rev. Lett.* **105**, 216407 (2010).
 - [27] Shin-ichi Kimura and Hidekazu Okamura, *J. Phys. Soc. Jpn.* **82**, 021004 (2013).
 - [28] R. J. Pressley, ed., "CRC Handbook of Laser with Selected Data on Optical Technology", Chemical Rubber Co. (1971).
 - [29] S. J. Moon, Hosub Jin, W. S. Choi, J. S. Lee, S. S. A. Seo, J. Yu, G. Cao, T. W. Noh, and Y. S. Lee, *Phys. Rev. B* **80**, 195110(2009).
 - [30] Hitoshi Seo, Jaime Merino, Hideo Yoshioka, and Masao Ogata, *J. Phys. Soc. Jpn.* **75**, 051009 (2006).
 - [31] D. Faltermeyer, J. Barz, M. Dumm, M. Dressel, N. Drichko, B. Petrov, V. Semkin, R. Vlasova, C. Mezière, and P. Batail, *Phys. Rev. B* **76**, 165113 (2007).
 - [32] T. Sasaki, I. Ito, N. Yoneyama, N. Kobayashi, N. Hanasaki, H. Tajima, T. Ito, and Y. Iwasa, *Phys. Rev. B* **69**, 064508 (2004).
 - [33] L. Degiorgi, G. Grüner, K. Kim, R. H. McKenzie, and P. Wachter, *Phys. Rev. B* **49**, 14754 (1994).
 - [34] T. Ivek, B. Korin-Hamzić, O. Milat, S. Tomić, C. Claus, N. Drichko, D. Schweitzer, and M. Dressel, *Phys. Rev. B* **83**, 165128 (2011).
 - [35] R. Okazaki, Y. Ikemoto, T. Moriwaki, T. Shikama, K. Takahashi, H. Mori, H. Nakaya, T. Sasaki, Y. Yasui, and I. Terasaki, *Phys. Rev. Lett.* **111**, 217801 (2013).
 - [36] Toshihiro Takahashi, Yoshio Nogami, and Kyuya Yakushi, *J. Phys. Soc. Jpn.* **75**, 051008 (2006).
 - [37] T. Katsufuji, T. Tanabe, T. Ishikawa, Y. Fukuda, T. Arima, and Y. Tokura, *Phys. Rev. B* **54**, R14230(R) (1996).
 - [38] Masayuki Tanaka, Kaoru Yamamoto, Mikio Uruichi, Takashi Yamamoto, Kyuya Yakushi, Shinya Kimura, and Hatsumi Mori, *J. Phys. Soc. Jpn.* **77**, 024714 (2008).
 - [39] K. Yakushi, *Crystals* **2**, 1291 (2012).
 - [40] Yue Yue, Kaoru Yamamoto, Mikio Uruichi, Chikako Nakano, Kyuya Yakushi, Shigeaki Yamada, Toshihiro Hiejima, and Atsushi Kawamoto, *Phys. Rev. B* **82**, 075134 (2010).
 - [41] Y. S. Lee, J. S. Lee, K. W. Kim, T. W. Noh, Jaeyun Yu, E. J. Choi, G. Cao, and J. E. Crow, *Europhys. Lett.*, **55**, 280-286 (2001).